JOURNAL OF GEOPHYSICAL RESEARCH, VOL. 103, NO. B9, PAGES 21,091–21,097, SEPTEMBER 10, 1998

Stress field associated with the rupture of the 1992 Landers, California, earthquake and its implications concerning the fault strength at the onset of the earthquake

Michel Bouchon and Michel Campillo

Laboratoire de Géophysique Interne et Tectonophysique, Université Joseph Fourier and Centre National de la Recherche Scientifique, Grenoble, France

Fabrice Cotton

Institut de Protection et de Sûreté Nucléaire, Fontenay aux Roses, France

Abstract. We investigate the space and time history of the shear stress produced on the fault during the 1992 Landers earthquake. The stress is directly calculated from the tomographic image of slip on the fault derived from near-source strong motion data. The results obtained shed some light on why the earthquake rupture cascaded along a series of previously distinct fault segments to produce the largest earthquake in California in over 40 years. Rupture on the 30 km long northernmost segment of the fault was triggered by a large dynamic increase of the stress field, of the order of 20 to 30 MPa, produced by the rupturing of the adjacent fault segments. Such a large increase was necessary to overcome the static friction on this strand of the fault, unfavorably oriented in today's tectonic stress field. This misorientation eventually led to the arrest of rupture. The same mechanism explains why rupture broke only a small portion of the Johnson Valley fault on which the earthquake originally started, before jumping to an adjacent fault more favorably oriented. We conclude from these results that the dynamic stress field could not sustain and drive the rupture along the strongly misoriented NW-SE strands of the preexisting fault system. Instead, the dynamic stress field produced new fractures favorably oriented in a N-S direction and connecting parts of the old fault system.

1. Introduction

Since the monumental work of *Reid* [1910] and his coworkers following the 1906 San Francisco earthquake, it is known that earthquakes are produced by the sudden release of stress in rocks. As most earthquakes occur along preexisting faults, the knowledge of the state of stress on faults is an important element to understand and eventually predict earthquakes. Direct measurements of stress at or near a fault are only possible at shallow depth and have led to results which are often difficult to conciliate with friction laws [*Zoback et al.*, 1987]. The detailed tomographic models of earthquake slip obtained in recent years for some large well-recorded events provide the means to indirectly infer some of the characteristics of the stress field acting on earthquake faults [*Quin*, 1990; *Miyatake*, 1992; *Mikumo and Miyatake*, 1995; *Bouchon*, 1997; *Ide and Takeo*, 1997]. In the present study we shall use this approach to investigate features of the stress field associated with the 1992 Landers, California, earthquake. We shall determine the spatio-temporal image of the shear stress produced on the fault, and we shall try to infer from this image some aspects of the dynamics of the rupture during the earthquake.

Paper number 98JB01982.
0148-0227/98/98JB-01982$09.00

2. Fault Slip

The 1992 Landers earthquake (M_w = 7.3) is the largest event which occurred in California in over 40 years. Its surface rupture extends along four previously distinct fault segments and across a series of complex fault intersections for about 80 km [*Hart et al.*, 1993; *Sieh et al.*, 1993] (Figure 1a). The earthquake generated an exceptional set of near-source seismic, geodetic, and radar-interferometry data. Inversions of some of these records to infer the space-time history of the rupture have been performed by *Wald and Heaton* [1994], *Cohee and Beroza* [1994], and *Cotton and Campillo* [1995]. We shall use here the results from the latter study which provides tomographic images of the rupturing fault in terms of slip, rupture time, and rupture duration.

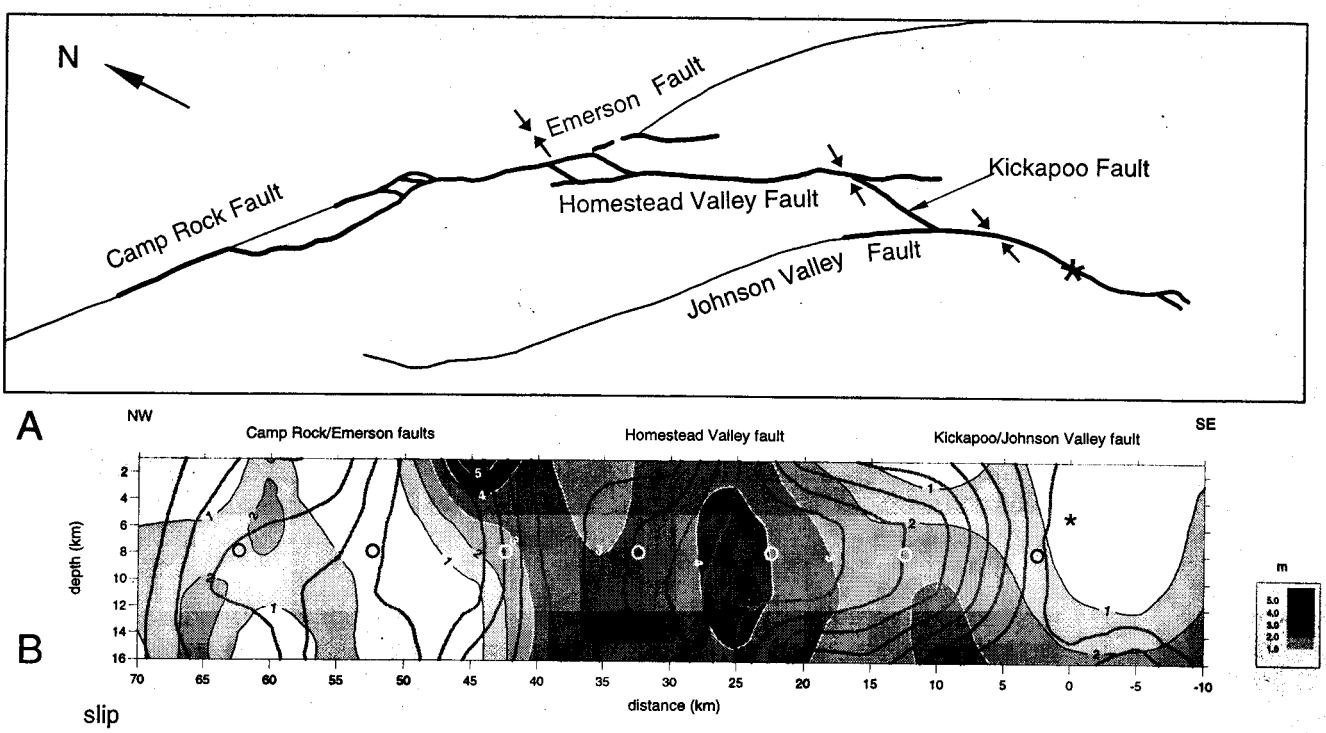

Figure 1. (a) Map of major faults (light solid line) and surface rupture (heavy solid line) produced during the Landers earthquake (simplified from *Hart et al.* [1993]). The arrows represent the orientation of the maximum pre-earthquake compression axis inferred by *Hauksson* [1994] from the 1975 Galway Lake sequence (near the Emerson fault), the 1979 Homestead Valley sequence, and the 1981 to 1991 background seismicity (shown near the Johnson Valley fault, where many of these events are located). (b) Spatial distribution of slip on the fault inferred by *Cotton and Campillo* [1995] and isochrones showing the position of the rupture front at 1 s time intervals. The hypocenter is denoted by a star. The circles show the location of the fault points considered in Figure 2.

The fault geometry itself is relatively well defined by the surface fractures and the aftershock locations [*Sieh et al.*, 1993; *Hauksson et al.*, 1993]. Its dip is nearly vertical and the rupture extends down to about 16 km. In the model of *Cotton and Campillo* [1995] the fault geometry is approximated by three vertical segments striking N6°W, N29°W, and N38°W and 25, 25, and 30 km long, respectively. Because the width of the shear zones connecting the different segments [e.g., *Johnson et al.*, 1994] is beyond the resolving power of the data, the connection between the faults is idealized, the extremity of one segment meeting the start of the next segment. The slip, shown in Figure 1b, is almost purely strike-slip and displays a strong spatial variation. It is relatively small (1 m or less) in the hypocentral area and reaches values of 3 to 5 m over a large portion of the fault before diminishing on the northernmost part of the fault. The position of the rupture front, depicted at 1 s intervals from the start of nucleation until the end of propagation about 22 s later, shows that rupture propagated over the fault at locally varying velocity. The duration of slippage inferred by *Cotton and Campillo* [1995] also varies greatly over the fault, ranging from 1 to 5 s.

3. Stress Images

From the slip space and time history one may directly calculate the temporal evolution of stress anywhere on the fault [*Bouchon*, 1997]. Results of this calculation at seven fault locations are displayed in Figure 2. The points considered are located at 8 km depth and are chosen to sample the fault at 10 km intervals (Figure 1b). The component of stress depicted is the horizontal shear stress which, the earthquake being almost purely lateral strike-slip, is by far the largest shear stress component acting on the fault. The time histories presented start at the time of rupture nucleation. The first stage corresponds, at all locations, to a gradual increase in shear stress above the initial stress level. This increase begins with the arrival of seismic waves from the hypocentral area. The shear stress reaches a peak just before rupture. Then, as sliding occurs, the stress begins to drop. At or near the end of sliding, it reaches a minimum level before increasing again to its final static value after the arrest of slip. Following *Quin* [1990] and *Miyatake* [1992], we denote the stress increase at the onset of rupture as the strength excess, which added to the

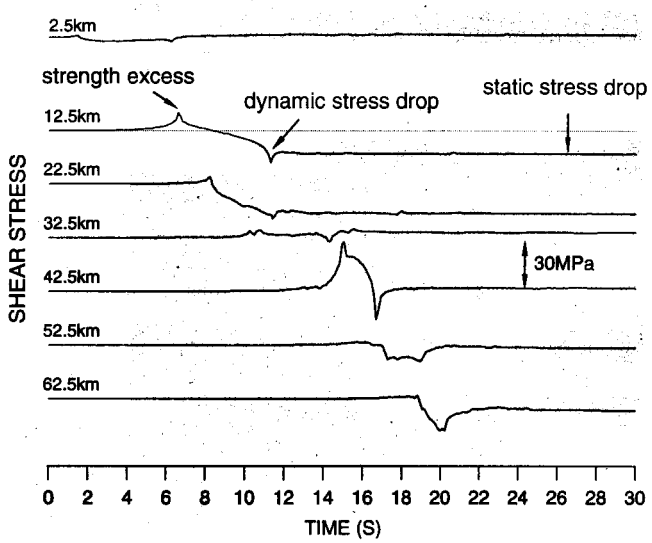

Figure 2. Time histories of shear stress at several fault locations. The fault points considered are at 8 km depth and at epicentral distances ranging from 2.5 to 62.5 km (see Figure 1b).

initial stress corresponds to the yield stress of the rock to fracture or, on a preexisting fault, corresponds to the static friction. Once the yield stress of the rock or the static friction is reached, rupture occurs and the stress drops. The dynamic stress drop corresponds to the largest drop from the initial shear stress level during the rupture process, while the static stress drop measures the change in stress produced by the earthquake.

Images of the spatial distribution of these three physical parameters over the fault are presented in Figure 3. The calculation takes into account the changes in fault orientation. We have excluded from these maps points located near the two sharp bends in the fault model geometry, located at 15 and 40 km, because at these bends, stress is discontinuous and that such a discontinuity is artificially imposed by the sharp change in fault orientation of the model. Instead, we have chosen to interpolate the stress values there from neighboring values, calculated less than 1 km away from these sharp corners.

As observed for other California events [*Bouchon*, 1997], the dynamic stress drop (Figure 3a) varies greatly over the fault. Patches of high dynamic stress drop where the decrease in shear stress can reach 50 MPa or more alternate with regions of relatively low stress drop (10 MPa or less). The dynamic stress drop is in excess of 20 MPa over about half of the fault. The static stress drop (Figure 3b) is, on average, about 40% lower than the dynamic stress drop. The low stress drop in the upper 2 km reflects the low rigidity of the sediments.

The spatial resolution of these images is controlled by the resolution of the slip model inferred from the data (about 5 km). The high degree of heterogeneity of stress drops over the fault observed at this scale may thus also exist at finer scales.

The spatial resolution of the slip model may also produce some artefacts on the stress images. In particular, the apparent spatial periodicity, which seems to occur on the images of Figure 3, may be due to or reinforced by the spacing used in the original slip model.

4. Fault Strength

The strength excess (Figure 3c) which represents the apparent strength of the fault at the onset of the earthquake is also highly heterogeneous. Its low level in the hypocentral region indicates that the tectonic stress there, before the earthquake, was close to the critical stress or the static friction. This finding is supported by observations made by *Hauksson et al.* [1993] that at least 25 foreshocks of $M1.3 - 3.0$ occurred within a couple of kilometers of the hypocenter during the 7 hours preceding the mainshock. This unusual foreshock swarm activity, spread over several hours, shows that the rupture had difficulty generating enough energy to sustain its propagation. This is consistent with the low dynamic stress drop inferred in the hypocentral region. *Dodge et al.* [1996] have made a detailed study of the foreshock sequence, from which they tentatively concluded that the foreshocks were the seismic expression, at fault geometric heterogeneities, of a nucleation process which occurred mostly aseismically over the hypocentral area. Our present results of low strength excess and low dynamic stress drop in the hypocentral region seem physically consistent with such a type of deformation. Isochrones showing the propagation of the rupture front over the fault are also displayed in Figure 3c. The timing of the initial phase of the earthquake (the first 1 or 2 s) is somewhat uncertain because the earthquake itself was preceded by a foreshock 2.5 s earlier [*Campillo and Archuleta*, 1993] which overlaps the earthquake records.

One characteristic feature of the spatial distribution of strength excess over the fault is its strong correlation with the local rupture velocity: rupture propagates at high velocity over areas of the fault where the strength excess is low and decelerates upon encountering regions where the strength excess is large. When rupture propagates across such zones its velocity drops considerably. While the average rupture velocity inferred by *Cotton and Campillo* [1995] is about 3.2 km/s, it may fall to around 1.5 km/s over high strength areas and may reach values close to 6 km/s over the low strength regions. Such a correlation has been observed for the 1979 Imperial Valley earthquake [*Bouchon*, 1997] where the high rupture velocity inferred locally by *Archuleta* [1984] occurs over fault areas where the strength excess is low.

One remarkable feature of the Landers earthquake, when compared with other events, is that its rupture cascaded along previously distinct fault strands separated by wide step-overs. The three major shear zones

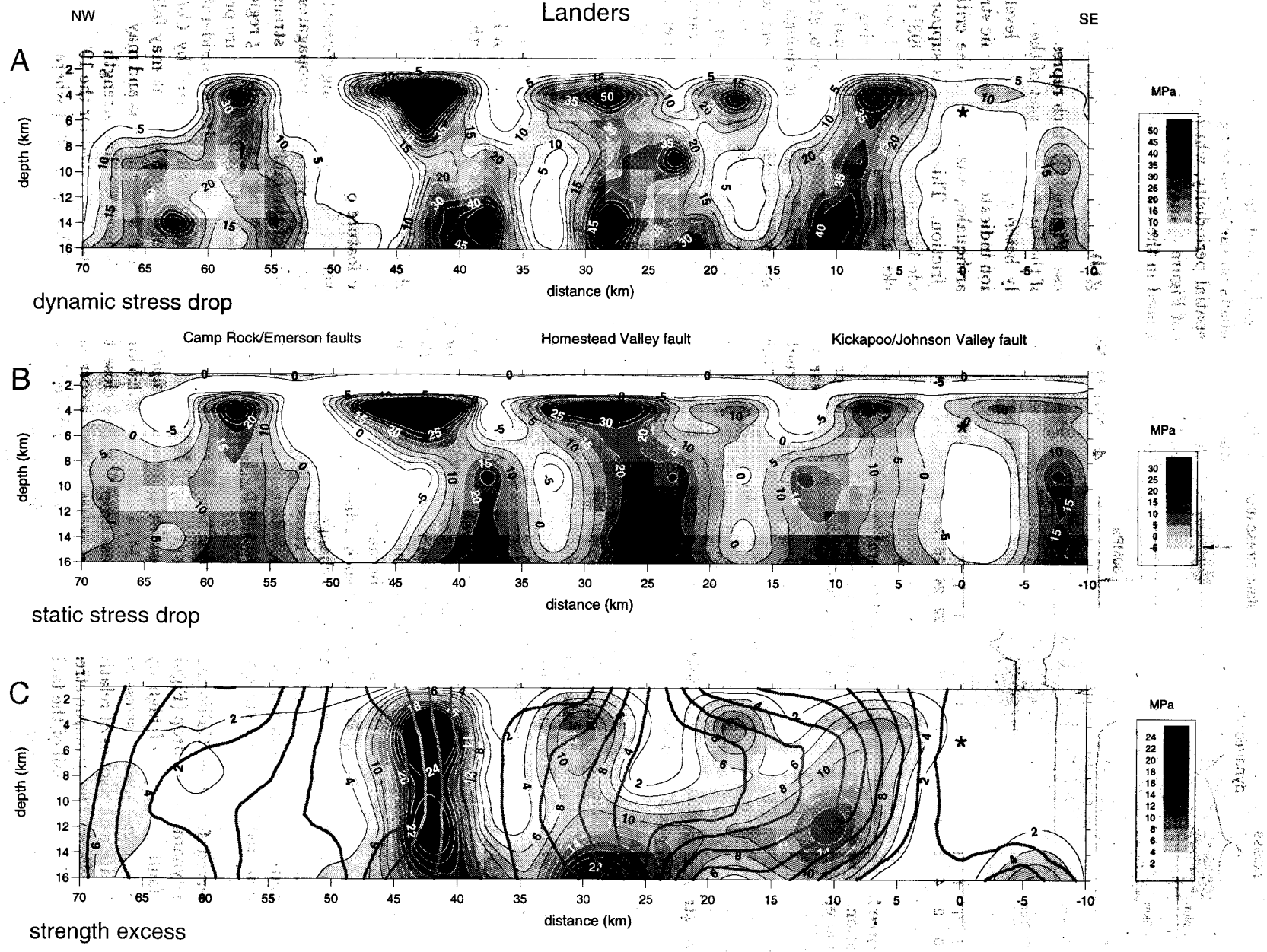
Landers
NW
SE
A
depth (km)
distance (km)
MPa
dynamic stress drop
Camp Rock/Emerson faults
Homestead Valley fault
Kickapoo/Johnson Valley fault
B
depth (km)
distance (km)
MPa
static stress drop
C
depth (km)
distance (km)
MPa
strength excess

connecting the individual fault segments are located between about 10 and 15 km from the epicenter (the Kickapoo fault connecting the Johnson Valley fault to the Homestead Valley fault), 35 to 40 km (the shear zone joining the Homestead Valley fault to the Emerson fault), and near 50-55 km (the Emerson to Camp Rock fault junction) (Figure 1a). Interestingly, these zones are not characterized by specially high values of strength excess but display levels similar to neighboring regions of the fault. This result shows that the propagation of the rupture along the 80 km fault zone was not significantly impeded by the presence of lateral offsets between the various fault strands. It suggests that the shear energy required to break these geometric barriers was of the same order as the energy level necessary to overcome static friction elsewhere on the fault. One possible explanation for this is that the fault segments were already connected at depth. An alternative interpretation is that the shear energy required to fracture intact rock was close to the one necessary to overcome friction. As the previous major rupture of these faults occurred several thousand years ago [*Sieh,* 1996], the long recurrence period may have given time to the fault to partially heal and regain a strength (static friction) close to the one of unbroken rock.

The region of highest strength excess is located between 40 and 45 km from the epicenter and corresponds to the beginning of rupture on the Emerson fault. There, compared to the previously ruptured fault segments, rupture suddenly takes a more northwesternly direction (Figure 1a). It has now rotated by about 30° from its original direction of nucleation and early propagation. This fault rotation occurs in a tectonic stress field where the spatial variations are small [*Hauksson,* 1994] (Figure 1a). Pre-earthquake stress orientation measurements made by *Hauksson* [1994], about 10 km away from the high-strength zone of the Emerson fault, using focal mechanisms from the 1975 Galway Lake earthquake sequence, yield a compression axis oriented around N26°E, that is at about 65° from the fault strike. By comparison, the direction of maximum compression in the hypocentral area prior to the earthquake is estimated to be between 35°and 40° from the fault strike [*Hauksson,* 1994].

In view of these observations, we interpret the high-strength zone at the beginning of seismic rupture on the Emerson fault as due to the unfavorable orientation of this fault in the regional tectonic stress field. A large increase in shear stress (of the order of 20 to 30 MPa) above the initial stress level is required for sliding to start on the Emerson fault. This large stress buildup is necessary to overcome the lower tectonic shear stress and the higher friction (reflecting the larger normal stress) on this fault segment. While the earthquake rupture could not have nucleated on this fault in the absence of fluid [*Scholz,* 1990; *Sibson,* 1990; *Hill and Thatcher,* 1992], rupture can be triggered there by the dynamic stress field generated by the rupturing of adjacent fault strands. This dynamic increase in shear stress is 2 orders of magnitude higher than regional stress changes induced by the earthquake and considered to be responsible for triggering some aftershocks on neighboring faults [*Harris and Simpson,* 1992; *Jaumé and Sykes,* 1992; *Stein et al.,* 1992; *King et al.,* 1994].

Dynamic models of earthquakes that present changes in fault orientation predict that while rupture may be initiated on unfavorably oriented fault segments by the dynamic stress field, it will eventually die off and come to a stop [*Bouchon and Streiff,* 1997]. That this is what happens in the Landers earthquake is suggested by the way in which rupture arrest occurs, in the middle of the Camp Rock fault, which constitutes the northwestern continuation of the Emerson fault and runs along the same direction [*Dokka and Travis,* 1990]. One might have expected the strength excess to stay high on the Camp Rock fault, up to where rupture stops, or the slip to die out earlier on this segment. The amount of slip there, however, is small. This, combined with the fact that it occurs at the end of the rupture process, also suggests that the strength excess there is not as well resolved as on the other parts of the fault.

It seems likely that the same mechanism of rupture arrest took place, earlier in the earthquake, on the Johnson Valley fault, where this structure bends from a nearly northern direction to a more northwestern orientation (Figure 1a). This bend of the Johnson Valley fault forced rupture to change course and to follow a more favorable northern direction (the new Kickapoo fault) toward the next fault segment (the Homestead Valley fault).

The time history of shear stress in the middle of the high-strength region of the Emerson fault is displayed in Figure 2 (at 42.5 km of epicentral distance). Although the buildup of shear stress before rupture is impressive, the final stress drop is almost null, which suggests a low level of initial shear stress. *Hauksson* [1994] has shown that the aftershock focal mechanisms, which generally agree with the main shock motion along the Johnson Valley, Kickapoo, and Homestead Valley faults, become complex and highly variable along the Emerson/Camp Rock rupture zone. Hauksson interpreted this heterogeneity of mechanisms as indicative of

Figure 3. (a) and (b) Spatial distributions of stress drop and (c) strength excess over the fault. The position of the hypocenter is indicated by a star, and the isochrones showing the location of the rupture front at 1 s time intervals are displayed in Figure 3c.

the almost complete release of shear stress there during the main shock. A similar explanation was proposed by *Beroza and Zoback* [1993] to account for the diversity of aftershock mechanisms following the 1989 Loma Prieta earthquake. The relatively small static stress drop on the Camp Rock/Emerson faults, which averages about 5 MPa below 5 km, thus confirms the low tectonic shear stress on these faults at the onset of the earthquake.

These results confirm the misorientation of the Emerson/Camp Rock faults in today's tectonic stress environment. They support the hypothesis advanced by *Nur et al.* [1993] that many of the older strike-slip faults in the region, referred to as the eastern California shear zone, have become unfavorably oriented with respect to the regional stress field and that crustal deformation is now shifting to a new throughgoing fault that cuts obliquely across them and runs approximately N15°W. This explanation of the unusual Landers sequence substantially differs from the one proposed by *Sieh* [1996], who attributes the arrest of rupture on the Camp Rock fault to the occurrence of a more recent earthquake there (2000 to 3000 years ago) than on the Landers/Homestead-Valley/Emerson segments where the last event is thought to have occurred between 6000 and 9000 years ago [*Hecker et al.*, 1993; *Rubin and Sieh*, 1993; *Rockwell et al.*, 1993]. As noted by *Sieh* [1996], however, pre-1992 failure cannot explain the rupture arrest on the northern Johnson Valley fault, as this fault has not failed for about 9000 years [*Herzberg and Rockwell*, 1993].

The validity of this analysis relies on the reliability of the slip model inferred from the near-source seismic records. In this respect a comparison of the model used here with those obtained by *Wald and Heaton* [1994] and *Cohee and Beroza* [1994] provides a useful estimate of the variability of models obtained using different inversion schemes and slightly different sets of data. The amplitude range and spatial distribution of slip on the fault inferred in these three studies are in good general agreement and should provide a similar pattern of stress drop heterogeneity and stress drop levels over the fault. The steep gradient in slip amplitude at the beginning of the Emerson fault is also well present in the three models. The slowing down in rupture velocity when rupture starts on the Emerson fault, which combined with the steep slip gardient there leads to the high strength estimate, is also a characteristic of *Wald and Heaton*'s [1994] model. Thus, although images will vary in detail, their major features should be relatively similar.

5. Conclusion

One of the most remarkable feature of the Landers earthquake is that its rupture cascaded along a series of distinct fault segments and across complex fault intersections to produce the largest earthquake in California in over 40 years. During this 80 km long propagation, rupture rotated by about 30°. Using tomographic images of the earthquake slip, we have shown that rupture on the 30 km long northernmost segment of the fault was triggered by the dynamic stress field generated by the rupturing of adjacent fault segments. This dynamic field increased the initial stress level on the first 5 km of this segment by about 20 to 30 MPa. Such a large increase was necessary to overcome friction on this unfavorably oriented strand of the fault, which lies at about 65° from the regional direction of maximum compression. This misorientation eventually led to the arrest of rupture. The same mechanism explains why rupture broke only a small portion of the Johnson Valley fault before jumping to an adjacent fault more favorably oriented.

Acknowledgments. This work benefited greatly from the numerous comments and suggestions of Greg Beroza, Mark Zoback, and David Wald.

References

Archuleta, R.J., A faulting model for the 1979 Imperial Valley earthquake, *J. Geophys. Res., 89,* 4559-4585, 1984.

Beroza, G.C., and M.D. Zoback, Mechanism diversity of the Loma Prieta afterschocks and the mechanics of mainschock afterschock interaction, *Science, 259,* 210-213, 1993.

Bouchon, M., The state of stress on some faults of the San Andreas system as inferred from near-field strong motion data, *J. Geophys. Res., 102,* 11731-11744, 1997.

Bouchon, M., and D. Streiff, Propagation of a shear crack on a nonplanar fault: A method of calculation, *Bull. Seismol. Soc. Am., 87,* 61-66, 1997.

Campillo, M., and R.J. Archuleta, A rupture model for the 28 June 1992 Landers, California earthquake, *Geophys. Res. Lett., 20,* 647-650, 1993.

Cohee, B.P., and G.C. Beroza, Slip distribution of the 1992 Landers earthquake and its implications for earthquake source mechanics, *Bull. Seismol. Soc. Am., 84,* 692-712, 1994.

Cotton, F., and M. Campillo, Frequency domain inversion of strong motions: Application to the 1992 Landers earthquake, *J. Geophys. Res., 100,* 3961-3975, 1995.

Dodge, D.A., G.C. Beroza, and W.L. Ellsworth, Detailed observations of California foreshock sequences: Implications for the earthquake initiation process, *J. Geophys. Res., 101,* 22371-22392, 1996.

Dokka, R.K., and C.J. Travis, Late cenozoic strike-slip faulting in the Mojave Desert, California, *Tectonics, 9,* 311-340, 1990.

Harris, R.A., and R.W. Simpson, Changes in static stress on southern California faults after the 1992 Landers earthquake, *Nature, 360,* 251-254, 1992.

Hart, E.W., W.A. Bryant, and J.A. Treiman, Surface faulting associated with the June 1992 Landers earthquake, California, *Calif. Geol., 46,* 10-16, 1993.

Hauksson, E., State of stress from focal mechanisms before and after the 1992 Landers earthquake sequence, *Bull. Seismol. Soc. Am., 84,* 917-934, 1994.

Hauksson, E., L.M. Jones, K. Hutton, and D. Eberhart-Phillips, The 1992 Landers earthquake sequence: Seismological observations, *J. Geophys. Res., 98,* 19835-19858, 1993.

Hecker, S., T.E. Fumal, T.J. Powers, J.C. Hamilton, C.D. Garvin, D.P. Schwatz, and F.R. Cinti, Late Pleistocene-Holocene behavior of the Homestead Valley fault segment,

1992 Landers, Ca surface rupture (abstract), *Eos Trans. AGU, 74 (43)*, Fall Meet. supl., 612, 1993.

Herzberg, M., and T. Rockwell, Timing of past earthquakes on the northern Johnson Valley fault and their relationship to the 1992 rupture (abstract), *Eos Trans. AGU, 74 (43)*, Fall Meet. supl., 612, 1993.

Hill, D.P., and W. Thatcher, An energy constraint for frictional slip on misoriented faults, *Bull. Seismol. Soc. Am., 82*, 883-897, 1992.

Ide, S., and M. Takeo, Determination of constitutive relations of fault slip based on seismic wave analysis, *J. Geophys. Res., 102*, 27379-27391, 1997.

Jaumé, S.C., and L.R. Sykes, Changes in state of stress on the southern San Andreas fault resulting from the California earthquake sequence of April to June 1992, *Science, 258*, 1325-1328, 1992.

Johnson, A.M., R.W. Fleming, and K.M. Cruikshank, Shear zones formed along long, straight traces of fault zones during the 28 June 1992 Landers, California, earthquake, *Bull. Seismol. Soc. Am., 84*, 499-510, 1994.

King, G.C.P., R.S. Stein, and J. Lin, Static stress changes and the triggering of earthquakes, *Bull. Seismol. Soc. Am., 84*, 935-953, 1994.

Mikumo, T., and T. Miyatake, Heterogeneous distribution of dynamic stress drop and relative fault strength recovered from the results of waveform inversion: The 1984 Morgan Hill, California, earthquake, *Bull. Seismol. Soc. Am., 85*, 178-193, 1995.

Miyatake, T., Reconstruction of dynamic rupture process of an earthquake with constraints of kinematic parameters, *Geophys. Res. Lett., 19*, 349-352, 1992.

Nur, A., H. Ron, and G.C. Beroza, The nature of the Landers-Mojave earthquake line, *Science, 261*, 201-203, 1993.

Quin, H., Dynamic stress drop and rupture dynamics of the October 1979 Imperial Valley, California, earthquake, *Tectonophysics, 175*, 93-117, 1990.

Reid, H.F., The mechanics of the earthquake, in *The California Earthquake of April 18, 1906, Report of the State Earthquake Investigation Commission*, vol. 2, 192pp., Carnegie Inst. of Washington, Washington, D.C., 1910.

Rockwell, T.K., D.P. Schwartz, K. Sieh, C. Rubin, S. Lindwall, M. Hertzberg, D. Padgett, and T. Fumal, Initial paleoseismic studies following the Landers earthquake: Implications for fault segmentation and earthquake clustering (abstract), *Eos Trans. AGU, 74 (43)*, Fall Meet. supl., 67, 1993.

Rubin, C., and K. Sieh, Long recurrence interval for the Emerson fault: Implications for slip rates and probabilistic seismic hazard calculations (abstract), *Eos Trans. AGU, 74 (43)*, Fall Meet. supl., 612, 1993.

Scholz, C.H., *The mechanics of Earthquakes and Faulting*, 439 pp., Cambridge Univ. Press, New York, 1990.

Sibson, R.H., Rupture nucleation on unfavorably oriented faults, *Bull. Seismol. Soc. Am., 80*, 1580-1604, 1990.

Sieh, K., The repetition of large-earthquake ruptures, *Proc. Natl. Acad. Sci. U.S.A., 93*, 3764-3771, 1996.

Sieh, K., et al., Near-field investigations of the Landers earthquake sequence, April to July 1992, *Science, 260*, 171-176, 1993.

Stein, R.S., G.C.P. King, and J. Lin, Change in failure stress on the southern San Andreas fault system caused by the 1992 magnitude=7.4 Landers earthquake, *Science, 258*, 1328-1332, 1992.

Wald, D.J., and T.H. Heaton, Spatial and temporal distribution of slip for the 1992 Landers, California, earthquake, *Bull. Seismol. Soc. Am., 84*, 668-691, 1994.

Zoback, M.D., et al., New evidence on the state of stress of the San Andreas fault system, *Science, 238*, 1105-1111, 1987.

M. Bouchon and M. Campillo, Laboratoire de Géophysique Interne et Tectonophysique, Université Joseph Fourier, IRIGM, BP 53X, 38041 Grenoble, France. (e-mail: Michel.Bouchon@obs.ujf-grenoble.fr; Michel.Campillo@obs.ujf-grenoble.fr)

F. Cotton, Institut de Protection et de Sûreté Nucléaire, BP 6, 92265 Fontenay aux Roses, France. (e-mail: Fabrice.Cotton@ipsn.fr)

(Received November 10, 1997; revised May 25, 1998; accepted June 2, 1998.)